
# Nano Scale Disruptive Silicon-Plasmonic Platform for Chip-to-Chip Interconnection

# Synthesis of Nanoparticles showing gain at 1550 nm

| | |
|---|---|
| Milestone no.: | M17 |
| Due date: | 10/31/2012 |
| Actual Submission date: | 10/31/2012 |
| Authors: | UGent |
| Work package(s): | WP4 |
| Distribution level: | RE[1] (NAVOLCHI Consortium) |
| Nature: | document, available online in the restricted area of the NAVOLCHI webpage |

## List of Partners concerned

| Partner number | Partner name | Partner short name | Country | Date enter project | Date exit project |
|---|---|---|---|---|---|
| 1 | Karlsruher Institut für Technologie | KIT | Germany | M1 | M36 |
| 2 | INTERUNIVERSITAIR MICRO-ELECTRONICA CENTRUM VZW | IMEC | Belgium | M1 | M36 |
| 3 | TECHNISCHE UNIVERSITEIT EINDHOVEN | TU/e | Netherlands | M1 | M36 |
| 4 | RESEARCH AND EDUCATION LABORATORY IN INFORMATION TECHNOLOGIES | AIT | Greece | M1 | M36 |
| 5 | UNIVERSITAT DE VALENCIA | UVEG | Spain | M1 | M36 |
| 6 | STMICROELECTRONICS SRL | ST | Italy | M1 | M36 |
| 7 | UNIVERSITEIT GENT | UGent | Belgium | M1 | M36 |

[1] **PU** = Public
**PP** = Restricted to other programme participants (including the Commission Services)
**RE** = Restricted to a group specified by the consortium (including the Commission Services)
**CO** = Confidential, only for members of the consortium (including the Commission Services)

## *Deliverable Responsible*

Organization: Ghent University
Contact Person: Zeger Hens
Address: Physics and Chemistry of Nanostructures
Krijgslaan 281-S3
B-9000 Gent
Belgium
Phone: +32 (0)9 – 2644863
Fax: +32 (0)9 – 264xxxx
E-mail: Zeger.Hens@UGent.be

## *Executive Summary*

## *Change Records*

| Version | Date | Changes | Author |
|---|---|---|---|
| 0.1 (draft) | 2012-01-26 | Start | Martin Sommer |
| 1 (submission) | 2012-01-31 | | Martin Sommer |

## *Introduction*

This milestone is a first step in the direction of making an integrated amplifier where colloidal quantum dots are used as a gain medium. Based on the existing expertise within the *Physics and Chemistry of Nanostructures* research group of UGent, it was decided:

- To use quantum dots (QDs) based on lead chalcogenides (PbX) since these can be easily tuned to have an emission wavelength at around 1550 nm.
- To analyze gain in these nanocrystals using the variable stripe length (VSL) setup at UVEG, where the nanocrystals are incorporated in a PMMA slab and deposited on SiO2 without or with an intermediate gold layer.

A drawback of using PbX based QDs is the 8-fold degeneracy of the HOMO and LUMO levels. This requires that each QD contains at least 4 excitons on average to have gain.[1] This requirement limits the gain lifetime to the ps range, since it has to compete with the very efficient Auger recombination of multiple excitons. The strategy followed here is to circumvent the limitation of 4 excitons/QD by heterostructure formation – similar to what was demonstrated for CdS/ZnSe core/shell QDs.[2]

## *Methods and Results*

### Overview

To form PbX based heterostructures, we decided to use Pb/Cd cationic exchange. Here, we start from initial CdS or CdSe quantum rods, which can be transformed either completely or partially into PbS or PbSe quantum rods in a two step process involving the formation of $Cu_2S$ or $Cu_2Se$ as an intermediate material (see Fig. 1).[3]

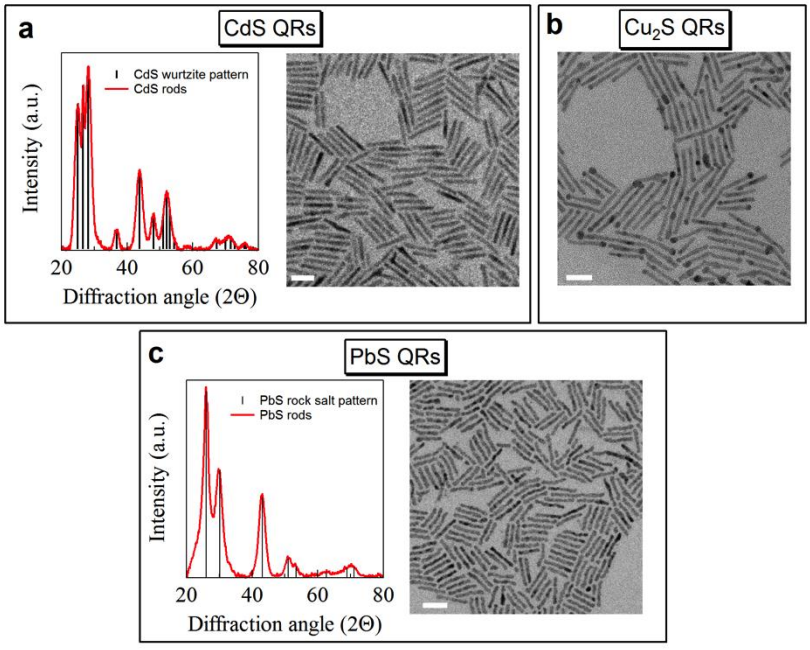


Figure 1: a) XRD difractrogram and TEM overview of the CdS QRs. b) TEM overview of Cu2S QRs. c) XRD and TEM overview of PbS QRs. All the scale bars are 20 nm.

The structures aimed at involve:

1. PbS/CdS quantum rods (QRs) made by (1) fully transforming an initial CdS rod into a PbS rod followed by (2) a partial re-exchange of Pb by Cd.
2. PbSe/CdSe quantum rods made by (1) fully transforming an initial CdSe rod into a PbSe rod followed by (2) a partial re-exchange of Pb by Cd.
3. PbS/CdS partially exchanged rods made by (1) partially transforming an initial CdS rod into a PbS/CdS rod where a single PbS dot is obtained at one side of the original CdS rod.

The resulting materials are typically characterized using structural analysis methods such as transmission electron microscopy (TEM) and optical methods such as absorption and luminescence spectroscopy.

**Synthesis of quantum rods**

*Initial PbX rod formation*. The starting materials are CdS or CdSe QRs, *e.g.*, synthesized with a seeded growth approach following Carbone et al.2 The successive Cd/Cu and Cu/Pb exchanges are promoted by methanol and tributylphosphine, respectively.[ref] Focusing on CdS rods with dimensions of (diameter:length) 3.7:28 nm (Figure 2a), we find that the successive exchange steps transform the absorption peak of the CdS bandgap transition at 480 nm to a shoulder at 1100 nm, which is characteristic of PbS (Figure 2b). Figure 2c shows that the PbS QRs thus formed are polycrystalline, with the different crystallites separated by [111] twin planes.

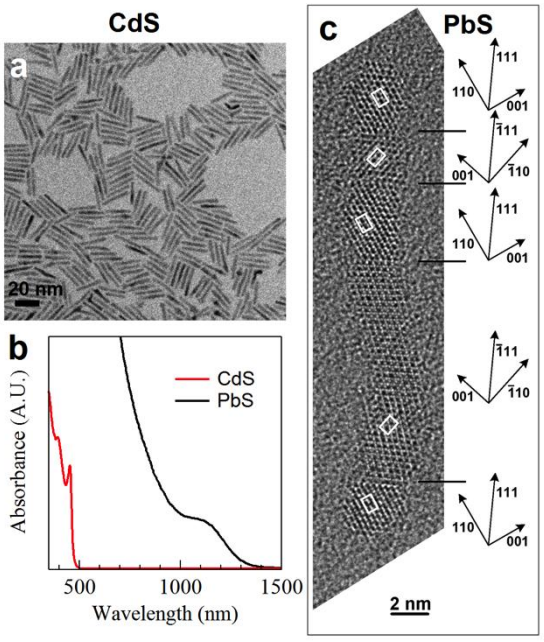


Figure 2: a) Overview TEM image of starting CdS QRs. b) Absorption spectra of CdS and PbS QRs from the same starting material. c) HR-TEM image of a PbS QR in [110] zone axis. The white rectangles indicate the <110> unit cell and the arrows show the three major crystal directions in the five crystal segments the rod is composed of.

*PbS/CdS multiple dot-in-rods*. In the case of PbX QDs, growth of a CdX shell by cationic exchange has been proposed as a way to enhance and stabilize the PLQY.[4,5] In line with this result, we have exposed a suspension of PbS QRs in toluene to an excess of Cd oleate at elevated temperature. Elemental analysis by TEM-EDX shows that this leads to a progressive replacement of Pb by Cd, which is more pronounced the longer the reaction time or the higher the temperature (Figure 3a). For exchange temperatures of 65 to 100°C, 45-95% of the Pb atoms are replaced by Cd, corresponding to a nominal shell thickness of 0.4-1.2 nm, respectively. As compared to the original PbS QRs, the PL spectrum of the PbS/CdS heterorods shifts to shorter

wavelengths and, more importantly, the PLQY increases sharply. After 120 min of shell growth, it reaches 45 or 55% if the exchange is done at 65 or 80°C, respectively (Figure 3b).

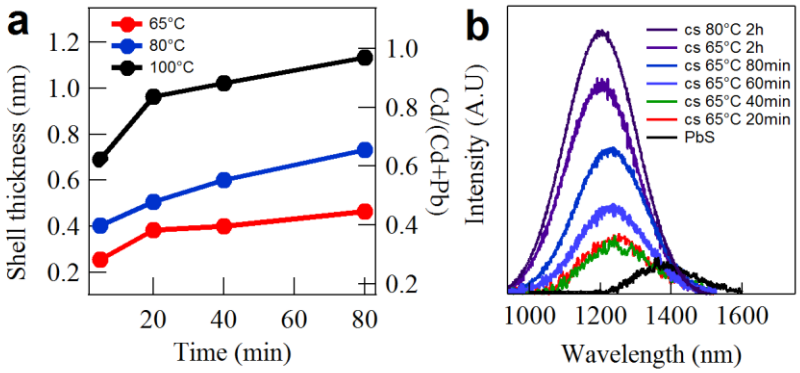


Figure 3: a) Evolution of the ratio Cd:Pb and the nominal CdS shell thickness as a function of the reaction time for different reaction temperatures . b) Evolution of the PL spectrum with the reaction time for an exchange reaction at 65°C and final PL spectrum for an exchange reaction at 80°C.

The morphology of the QRs was studied in detail using STEM-HAADF. With core/shell PbS/CdS heterorods, this should result in images showing a bright (PbS) core and a darker (CdS) shell. This is not what is observed. For QRs with dimensions 3.7:28 nm, with the final Pb for Cd exchange done at 65°C, the overview image (Fig. 4a) already shows that each rod is composed of a series of brighter and darker segments, featuring 4-5 bright parts. Fig. 4b demonstrates that the bright segments are embedded in the darker rod. We interpret this as evidence for the formation of multiple PbS dots in a single CdS rod. Similar results are obtained when starting from CdS rods with different aspect ratios.

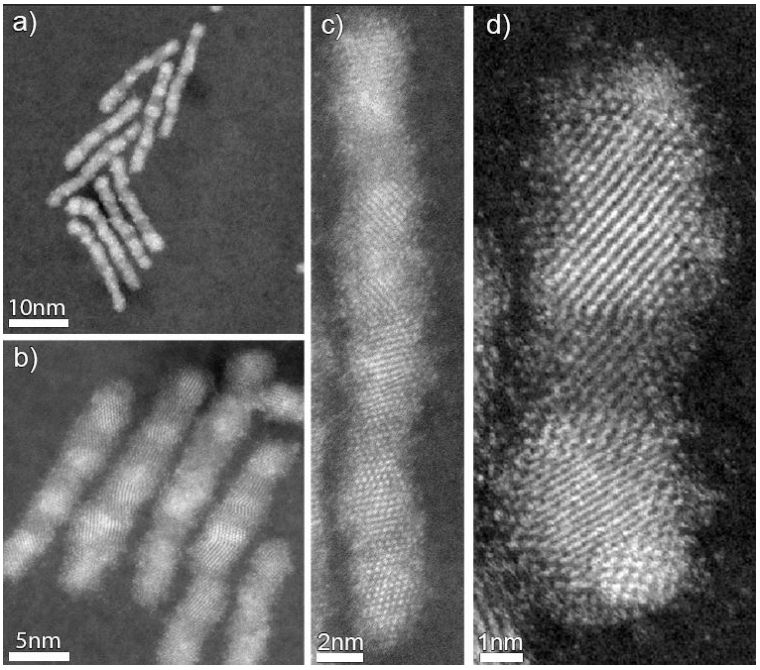


Figure 4: STEM-HAADF images of PbS/CdS rods showing multiple PbS QDs inside the rods recorded on a), b) and c) 3.7:28 nm QRs and (d) 4x14 nm QRs.

*PbSe/CdSe multiple dot-in-rods.* Here, we follow exactly the same procedure as with PbS/CdS multiple dot-in-rods, except that we start initially with CdSe QRs. Similar to PbS/CdS, we find that the final re-exchange of Pb for Cd results in the formation of multiple PbSe dots embedded in a single CdSe rod (see Fig. 5). Importantly, we find that the multiple PbSe/CdS dot-in-rods are more easily tuned to emit around 1550 nm.

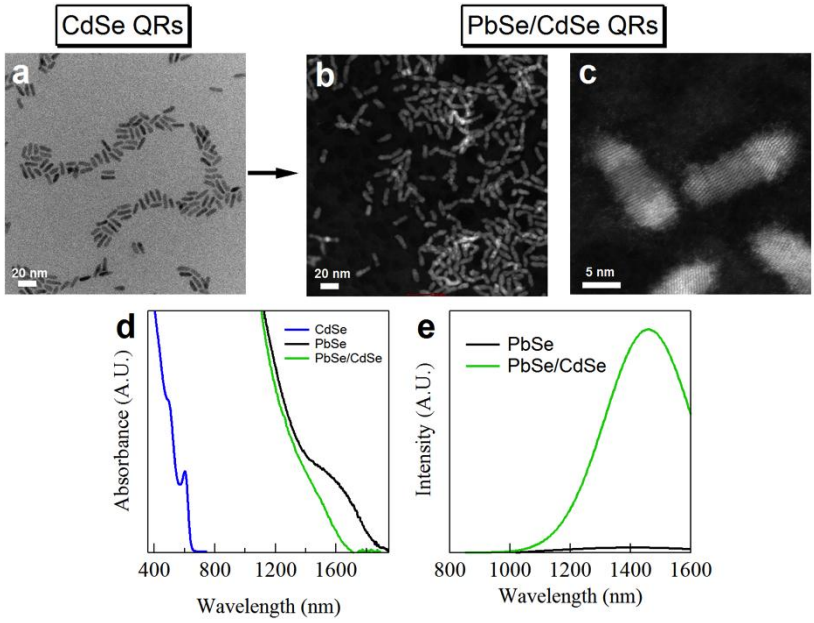


Figure 5: a) CdSe rods. b), c) STEM-HAADF pictures of PbSe/CdSe rods after the cationic exchange. c) Absorption spectra of the QRs at the different steps of the cationic exchange. d) Comparison of the PL intensity of the PbSe and PbSe/CdSe QRs exchanged at 40°C for 2hours.

*PbS/CdS partially exchanged rods*. It has been shown in the literature that the Cd for Cu cationic exchange that lies at the basis of PbS rod formation can be limited such that only part of Cd is replaced by Cu. Here, we controlled the cationic exchange such that only a single $Cu_2S$ crystallite is formed at one side of the original CdS rod. After the Cu for Pb cationic exchange step, this results in PbS/CdS heterorods where a single PbS QD is found a tone side of a CdS QR (see Fig. 6).

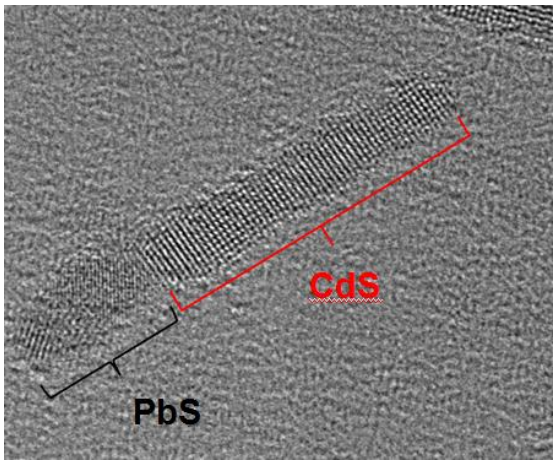


Figure 6: HR-TEM picture of a PbS/CdS partially exchanged rod.

### Transient absorption spectroscopy

We evaluate the potential for optical gain using femtosecond transient absorption (TA) spectroscopy. In this pump/probe experiment, the sample is excited using a (non-resonant, typically 700 nm) femtosecond pulse. After this photoexcitation, the change in absorption $\Delta a$ is monitored using a broadband (i.e. ‚white'), femtosecond probe pulse generated using a sapphire plate.

Optical transparency is reached when the normalized bleach satisfies:

$$\Delta a / a_0 = -1$$

Which is called the ‚transparency threshold'. Crossing this threshold (by increasing the excitation rate,i.e. the number of excitons (e-h pairs) per quantum dot) implies more photons are emitted at a certain wavelength than absorbed at that wavelength. This is necessary to achieve optical amplification in thin films. Using this method, we obtained both the spectral and temporal behaviour of the band-edge bleach.

### Spherical PbS nanocrystals

Using the femtosecond TA technique, we evaluate the potential of regular spherical PbS nanocrystals for optical amplification. These particles show very fast Auger recombination of multi-excitons required for population inversion in the degenerate (8-fold in both conduction and valence band) electronic structure of PbS.

As is evident from figure 7 (right), the normalized bleach never reaches transparency, even for the highest pump fluences. Also, the time traces in figure 7 (left) indicate a very short-lived multi-exciton population, decaying within 100 ps to the single exciton level (lifetime of single excitons is around 1 microsecond).

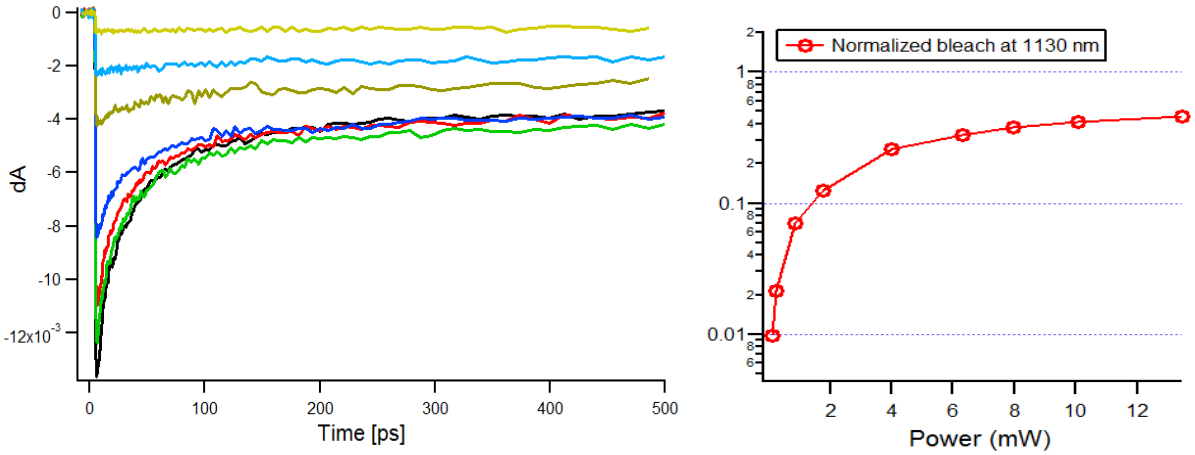


**Figure 7:** Spherical PbS nanocrystals - (left) Band edge bleach for increasing pump fluence as a function of time and (right) absolute value of normalized bleach as a function of pump fluence (equivalently pulse energy or average number of excitons per dot).

### PbS nanorods (12 nm x 4 nm x 4 nm)

We also investigated rod-shaped PbS nanocrystals. These particles have a much higher absorption cross section (owing to their larger volume and decreased electromagnetic screening)

leading to much higher excitation densities. In particular, up to 45 excitons per rod can be provided using similar fluences as in the dot-experiments.

Contrary to the spherical particles, these rod-shaped PbS nanocrystals do cross the transparency threshold over a wide wavelength range (1300 nm -1420 nm) which can be tuned to 1550 nm using rods with larger diameters.

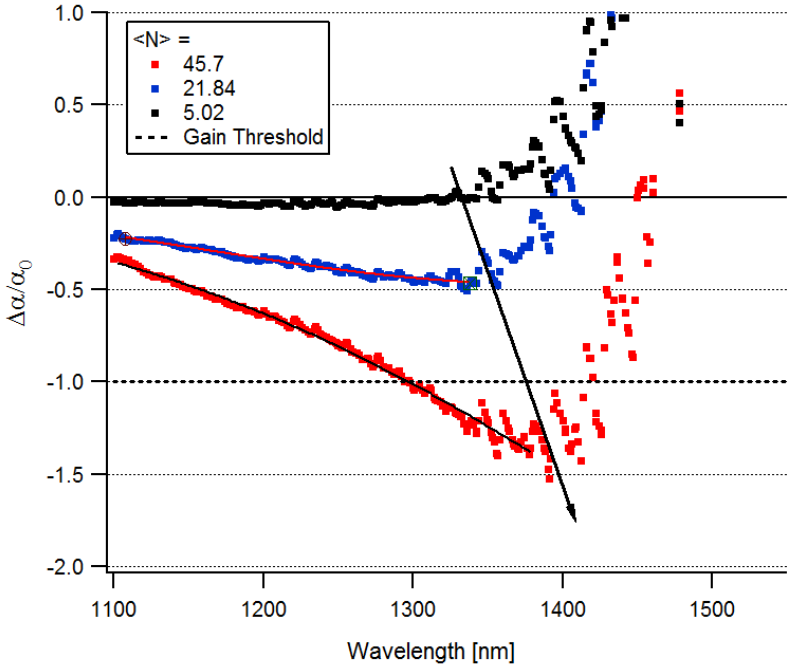


**Figure 8:** Normalized bleach spectrum for increasing pump fluence (or average number of excitons <N> per rod) for PbS nanorods.

Time traces of this bleach signal show that also in the PbS nanorods ultrafast Auger recombination still occurs. Typically, the transparency holds for only 10-15 ps.

Based on these results, we can asses that optical amplification using spherical PbS particles is not possible, whereas this would be possible with PbS rod-shaped particles. However, this requires high excitation densities typically not achievable under CW excitation.

## Gain measurements

To evaluate optical gain in nanocomposites (see MS16 report), the pumping scheme shown in figure 2 is used. This method is known as the variable stripe length method (VSL). In this setup, the pump laser is focused on the top surface of the sample with a cylindrical lens forming a stripe line. In order to provide a constant power in the whole stripe sides the laser spot was cut with a slit determining a stripe length of about 1.4 mm (Figure 2b). Then, it is possible to study the dependence of the waveguided PL by controlling the length of the stripe, and the absorption losses by keeping the length of the stripe constant and increasing its distance from the edge of the sample. In our case both experiments have been carried out moving the laser from the edge to the middle of the sample varying the parameter distance *x* of figure 2.b. So, during the first 1.4 mm (length of the stripe) waveguided PL is analyzed as a function of the length of the stripe. Then, the whole stripe is focused on the sample and PL is measured as a function of the distance between the stripe and the edge of the sample.

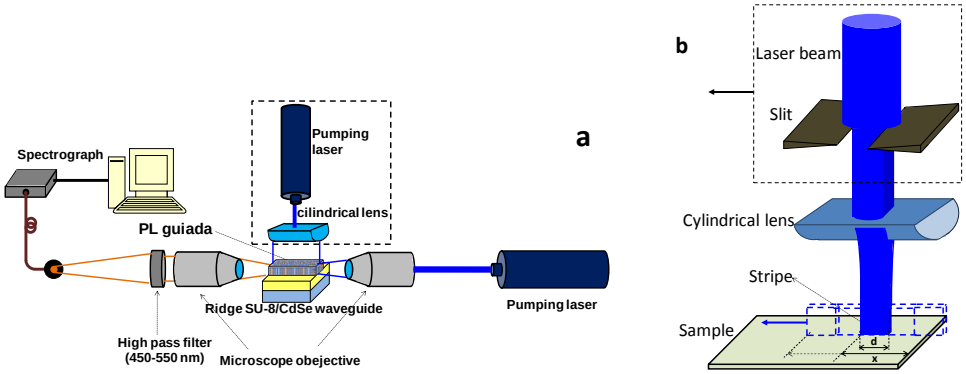


**Figure 2. a)Experimental set-up. b) Detail of the stripe movement**

The intensity of PL ($I_v$) is governed by the following equation:

$$\frac{dI}{dx} = I_{SS}(x) + (g(x) - a) \times I(x) \quad (1)$$

where $I_{ss}(x)$ is the intensity of spontaneous emission, $g$ the gain and $\alpha$ the losses and $x$ the horizontal distance. In the case where $g$ and $I_{ss}$ do not depend on $x$, equation (3) can be easily integrated to the general formula used in the VSL method:

$$I(x) = \frac{I_{ss}}{g - a}(e^{(g-a)x} - 1) \qquad (2)$$

However, although equation (2) is simple it doesn't take in account the saturation of PL observed in the experiments. For this purpose, it is necessary to include a saturation term with the horizontal distance in the gain coefficient. In the literature, saturation is modeled with the equation:

$$g(x) = \frac{g_0}{1 + \frac{I(x)}{I_{sat}}} \qquad (3)$$

where $g_0$ is the gain in $x = 0$ and $I_{sat}$ is the intensity of light during saturation. However this model does not reproduce well the sharp saturation trend observed in our experiments. On the contrary, the dependence of the gain can be nicely fitted if an exponential function is assumed:

$$g(x) = g_0 e^{-x/L} \quad (4)$$

where $L$ is a fitting parameter. It is not clear at this point how to interpret this quantity as it is typically introduced in pulsed measurements, reflecting the spatial spread of gain (or population inversion) under a pulsed pump source. The latter is not the case for our current experiments so care must be taken on how to interpret L. However, the data can be very well fit using the previous assumptions, allowing us to extract both initial gain $g_0$ and saturation length L.

Different nanocomposites were made typically by dissolving a given quantity of PbX/CdX – material in a PMMA stock solution. After sonication, these solutions were spincoated on glass or glass/metal substrates.

**PbS-CdS QRs**

| | absorption | UV-1400 nm | | emission | 1000-1600 nm | |
|---|---|---|---|---|---|---|
| **sample** | **ff** | **PMMA:QR** | **n 1100 nm** | **d (μm)** | **λ (nm)** | **Waveguiding** |
| A | $8\cdot10^{-4}$ | 1:0.1 | 1.4838 | 1.1 | - | all λ |
| B | $8\cdot10^{-3}$ | 1:1 | 1.4907 | 1.7 | 1270 nm | λ>633 nm |
| C | $4\cdot10^{-2}$ | 1:5 | 1.5214 | 1.2 | 1350 nm | λ>1100 nm |

**PER QRs**

| | absorption | UV-1000 nm | | emission | 900-1600 nm | |
|---|---|---|---|---|---|---|
| | **ff** | **PMMA:QR** | **n 1100 nm** | **d (μm)** | **λ (nm)** | **Waveguiding** |
| D | $1\cdot10^{-2}$ | 1:1 | 1.497 | 1.6 | 1250 nm | λ>633 nm |
| E | $8\cdot10^{-2}$ | 1:5 | 1.5594 | 1.6 | 1100 nm | λ>1100 nm |

**PbSe-CdSe QRs**

| | absorption | UV-1400 nm | | emission | 1000-1700 nm | |
|---|---|---|---|---|---|---|
| | **ff** | **PMMA:QR** | **n 1100 nm** | **d (μm)** | **λ (nm)** | **Waveguiding** |
| F | $9\cdot10^{-3}$ | 1:1 | 1.4938 | 1.6 | - | all λ |
| G | $4\cdot10^{-2}$ | 1:5 | 1.5306 | 1.6 | 1300 nm | λ>1100 nm |

**Table 1:** Nanocomposite materials used for VSL experiments.

Samples with different filling factors (ff) were analyzed using the VSL method as described above, both in a dielectric and plasmonic configuration. The main results of these measurements are summarized below for the different material systems investigated in this work. For the 'plasmonic' configurations, a distinction between TE and TM polarization of the collected waveguided light was made as plasmonic modes are expected to be purely TM polarized.

**PbS/CdS rods** - sample C, dielectric (left) and plasmonic (right)

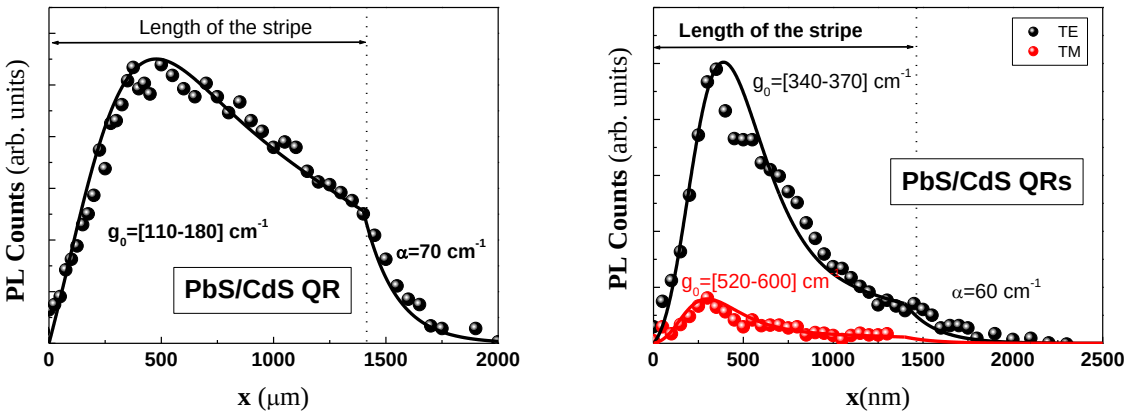

**PbS/CdS Partially Exchanged Rods (PER)** - sample D, dielectric (left) and plasmonic (right)

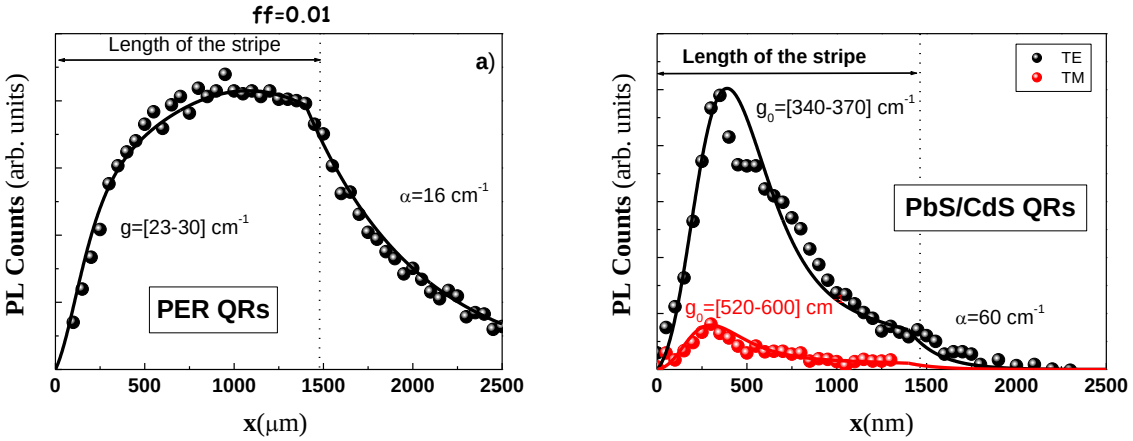


**PbSe/CdSe rods** – sample F, dielectric (left) and plasmonic (right)

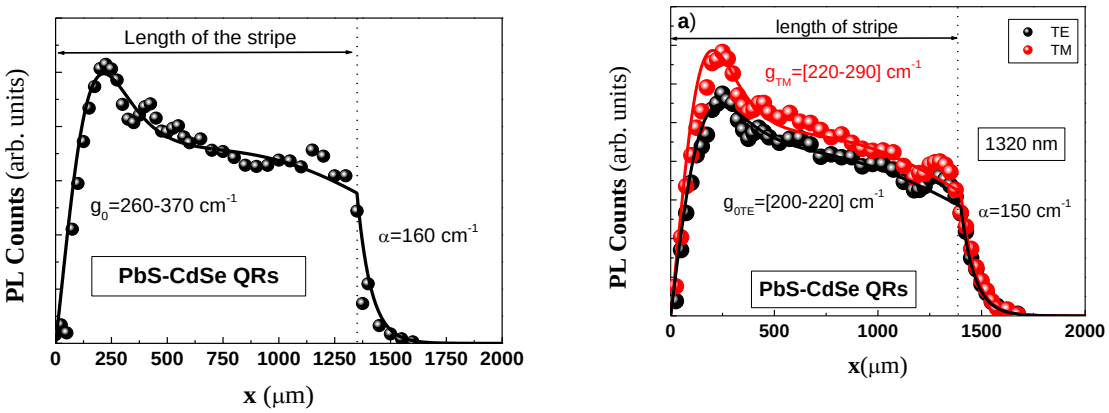


Modal gain values close to $200\,cm^{-1}$ were obtained depending on filling factor and polarization of waveguided light. Saturation lengths were typically close to 0.5 mm.

## *conclusion*

Transient absorption spectroscopy on PbS quantum rods has shown the occurrence of ASE in the wavelength range 1300-1420 nm. By adjusting the quantum rod synthesis, this can be shifted to 1550 nm. A drawback of the obtained result is the short gain lifetime, which makes CW gain impossible to reach.

To overcome this, more complex PbX/CdX heteronanostructures have been synthesized and analyzed for optical amplification using the VSL method, which indicate the presence of optical gain in all samples. We remain however carful in the interpretation of these results since VSL is a technique sensitive to measurement artifacts. As a next step, a transient absorption spectroscopy study is planned with the PbX/CdX heteronanostructures as well.

1 Schaller, R. D., Petruska, M. A. & Klimov, V. I. Tunable near-infrared optical gain and amplified spontaneous emission using PbSe nanocrystals. *Journal of Physical Chemistry B* 107, 13765-13768, doi:10.1021/jp0311660 (2003).
2 Klimov, V. I. *et al.* Single-exciton optical gain in semiconductor nanocrystals. *Nature* 447, 441-446 (2007).
3 Luther, J. M., Zheng, H. M., Sadtler, B. & Alivisatos, A. P. Synthesis of PbS Nanorods and Other Ionic Nanocrystals of Complex Morphology by Sequential Cation Exchange Reactions. *Journal of the American Chemical Society* 131, 16851-16857, doi:10.1021/ja906503w (2009).
4 Pietryga, J. M. *et al.* Utilizing the Lability of Lead Selenide to Produce Heterostructured Nanocrystals with Bright, Stable Infrared Emission. *Journal of the American Chemical Society* 130, 4879-4885 (2008).
5 Lambert, K., Geyter, B. D., Moreels, I. & Hens, Z. PbTe|CdTe Core|Shell Particles by Cation Exchange, a HR-TEM study. *Chemistry of Materials* 21, 778-780, doi:doi:10.1021/cm8029399 (2009).